Published in final edited form as:
Cardiogenetics. ; 1(1): .

LQTS-associated mutation A257G in α1-syntrophin interacts with the intragenic variant P74L to modify its biophysical phenotype

Jianding Cheng[1,2], **David W. Van Norstrand**[3], **Argelia Medeiros-Domingo**[3,4], **David J. Tester**[3,4], **Carmen R. Valdivia**[1], **Bi-Hua Tan**[1], **Matteo Vatta**[5], **Jonathan C. Makielski**[1], and **Michael J. Ackerman**[3,4]

[1]Division of Cardiovascular Medicine, Department of Medicine, University of Wisconsin, Madison, WI, USA

[2]Department of Forensic Pathology, Zhongshan School of Medicine, Sun Yat-sen University, Guangzhou, Guangdong, China

[3]Department of Molecular Pharmacology & Experimental Therapeutics, Mayo Clinic, Rochester, MN

[4]Departments of Medicine and Pediatrics, Mayo Clinic, Rochester, MN

[5]Section of Pediatric Cardiology, Texas Children's Hospital/Baylor College of Medicine, Houston, TX, USA

Abstract

The *SNTA1*-encoded α1-syntrophin (SNTA1) missense mutation, p.A257G, causes long QT syndrome (LQTS) by pathogenic accentuation of Nav1.5's sodium current (I_{Na}). Subsequently, we found p.A257G in combination with the SNTA1 polymorphism, p.P74L in 4 victims of sudden infant death syndrome (SIDS) as well as in 3 adult controls. We hypothesized that p.P74L-SNTA1 could functionally modify the pathogenic phenotype of p.A257G-SNTA1, thus explaining its occurrence in non-LQTS populations. The SNTA1 variants p.P74L, p.A257G, and the combination variant p.P74L/p.A257G were engineered using PCR-based overlap-extension and were co-expressed heterologously with SCN5A in HEK293 cells. I_{Na} was recorded using the whole-cell method. Compared to wild-type (WT), the significant increase in peak I_{Na} and window current found with p.A257G was reversed by the intragenic variant p.P74L (p.P74L/p.A257G). These results report for the first time the intragenic rescue of an LQT-associated SNTA1 mutation when found in combination with the SNTA1 polymorphism p.P74L, suggesting an ever-increasing picture of complexity in terms of genetic risk stratification for arrhythmia.

Keywords

long-QT syndrome; genetics; ion channels; SCN5A; syntrophin

Correspondence: Michael J. Ackerman, Department of Molecular Pharmacology & Experimental Therapeutics; Departments of Medicine and Pediatrics, Mayo Clinic, Rochester, MN 55905, USA. Tel. +1.507.284.0101 - Fax: +1.507.284-3757. ackerman.michael@mayo.edu.

Contributions: JC and DWVN contributed equally to this work.

Introduction

Long QT syndrome (LQTS) is a heritable cardiac arrhythmia affecting approximately 1 in 2500 individuals.[1] LQTS is characterized by a prolongation of the QT interval on the ECG, and is most often manifested clinically as syncope, seizures, or sudden death due to its trademark arrhythmia torsades de pointes.[2] Thus far, 12 genes have been implicated in LQTS, with approximately 75%[3,4] of LQTS caused by mutations in the KCNQ1-encoded potassium channel (LQT1),[5] KCNH2-encoded potassium channel (LQT2)[6] or the SCN5A-encoded sodium channel (LQT3).[7] Recent studies have also suggested that up to 10% of sudden infant death syndrome (SIDS) may be due to early manifestations of LQTS or other cardiac channelopathies during the first year of life.[8-16]

Recently, we discovered that the LQT3-associated cardiac sodium channel, Nav1.5, is connected by the SNTA1-encoded scaffolding protein (α1-syntrophin, SNTA1) to neuronal nitric oxide synthase (nNOS) and the cardiac iso-form of the plasma membrane Ca-ATPase (PMCA4b) in a complex in cardiomyocytes. Moreover, we implicated SNTA1 as a novel susceptibility gene for both LQTS[17] and SIDS[16] whereby the SNTA1 mutant disrupted binding with PMCA4b, released inhibition of nNOS, and accentuated both peak and late I_{Na} via Snitrosylation of the cardiac sodium channel. In addition we also have reported a new LQTS-associated SNTA1 missense mutation (c.770C > G, p.A257G) which precipitated a marked increase in peak I_{Na} and altered Nav1.5 channel kinetics in both HEK293 cells and cardiomyocytes through direct interaction of mutant SNTA1 with SCN5A.[18] All these findings suggest that SNTA1 is a crucial Nav1.5 channel interacting protein (ChIP) involved in maintaining the normal function of the cardiac sodium channel.

The p.A257G-SNTA1 mutation was identified initially in a separate publication by our group in 3 unrelated LQTS probands out of 39 LQTS patients but absent in 200 ethnic-matched control individuals.[18] This study demonstrated that p.A257G-SNTA1 can functionally interact with SCN5A in HEK293 cells without requiring nNOS or PMCA4b. Lastly, in a population-based cohort of 292 SIDS cases, we reported in 4 Caucasian SIDS victims the presence of p.A257G in combination with another single-nucleotide alteration (c. 221C > T) that results in the amino acid substitution p.P74L.[16] Interestingly, the combined variant of p.P74L/p.A257G was also found in 3 out of 400 additional adult controls not included in the initial study. None of the SIDS cases or the 400 adult controls was positive for either p.P74L- or p.A257G-SNTA1 in isolation.[16]

Given the following data points: i) that p.A257G-SNTA1 in isolation is an LQTS-associated mutation with abnormal biophysical characteristics,[18] ii) that p.A257G-SNTA1 was identified in an ostensibly healthy population only in the presence of p.P74L-SNTA1, and iii) that in an *at-risk* population of SIDS victims p.A257G-SNTA1 occurred multiple times, but only in the presence of p.P74L-SNTA1, we hypothesized that p.P74L may *rescue* the abnormal phenotype caused by p.A257G in isolation, therefore explaining its occurrence both in the general population compared to the LQT-associated single p.A257G missense mutation in isolation, as well as its occurrence at a higher frequency (>1%) in SIDS than would be expected were the combination p.P74L/p.A257G-SNTA1 variant to be a highly pathogenic variant.

Materials and Methods

Plasmid constructions of mammalian expression vectors

The cDNA (GenBank Accession no. NM_003098) of wild type (WT) human SNTA1 gene was subcloned into the pIRES2EGFP plasmid vector (Clontech Laboratories, Palo Alto, California, USA). The p.P74L-, p.A257G-, and combination p.P74L/p.A257G-SNTA1

variants were incorporated into WT-SNTA1 using the PCR-based overlap-extension method as previously reported.[16,17] All clones were sequenced to confirm integrity and to ensure the presence of the introduced variants and the absence of other substitutions caused by PCR.

Mammalian cell transfection

The WT or mutant SNTA1 in pIRES2EGFP vector was transiently co-transfected with expression vectors containing SCN5A (hNav1.5, Genbank accession no. AB158469) in the dominant splice variant background Q1077del into HEK293 cells with FuGENE6 reagent (Roche Diagnostics, Indianapolis, Indiana, USA) according to manufacturer's instructions. Cells were selected for electrophysiologic studies based on comparable levels of GFP fluorescence, and WT and mutant were transfected on the same day.

Electrophysiological measurements

Macroscopic voltage-gated I_{Na} was measured 48 hours after transfection with the standard whole-cell patch clamp method at 21°C to 23°C in the HEK293 cells. The extracellular (bath) solution contained the following (in mM): NaCl 140, KCl 4, $CaCl_2$ 1.8, $MgCl_2$ 0.75 and HEPES 5 and was adjusted to pH 7.4 with NaOH. The intracellular (pipette) solution contained the following (in mM): CsF 120, $CsCl_2$ 20, EGTA 2, NaCl 5, and HEPES 5 and was adjusted to pH 7.4 with CsOH. Microelectrodes were manufactured from borosilicate glass using a puller (P-87, Sutter Instrument Co, Novato, California, USA) and were heat polished with a microforge (MF-83, Narishige, Tokyo, Japan). The resistances of microelectrodes ranged from 1.0 to 2.0 MΩ. Voltage clamp data were generated with pClamp software 10.2 and an Axopatch 200B amplifier (Axon Instruments, Foster City, California, USA) with series-resistance compensation. Membrane current data were digitalized at 100 kHz, low-pass filtered at 5 kHz, and then normalized to membrane capacitance.

Persistent or late I_{Na} was measured as the mean between 600 and 700 ms after the initiation of the depolarization from -140 mV to -20 mV for 750 ms after passive leak subtraction as previously described.[13,16,17,19] Time course of recovery from inactivation was analyzed by fitting data with a two-exponential (exp) function: normalized $I_{Na}(t) = A_f [1 - \exp(-t/\tau_f)] + A_s [1 - \exp(-t/\tau_s)]$, where t is time, A_f and A_s are fractional amplitudes of fast and slow components, respectively, and τ_f and τ_s are fast and slow time constant, respectively. Decay rates and amplitude component were measured from the trace beginning after peak I_{Na} at 90% of peak I_{Na} to 24 ms and fitted with a sum of exponentials(exp): $I_{Na}(t) = 1 - [A_f \exp(-t/\tau_f) + A_s \exp(-t/\tau_s)]$ + offset, where t is time, and A_f and A_s are fractional amplitudes of fast and slow components, respectively. The other standard voltage clamp protocols are presented with the data and data were measured and analyzed as described previously[13,16,17,19] and with additional details provided in the figure legends. Quantification of window currents was performed by calculating the area under the activation/inactivation curves per cell, and averaging cells for each group to assess for statistical differences.

Statistical analysis

All data points are reported as the mean value and the standard error of the mean (SEM). Determinations of statistical significance were performed using a Student *t*-test for comparisons of two means or using analysis of variance (ANOVA) for comparisons of multiple groups. Statistical significance was determined by a value of $P < 0.05$.

Results

HEK293 cells were transiently transfected with Nav1.5 and either WT-SNTA1, p.P74LSNTA1, p.A257G-SNTA1, or p.P74L/p.A257GSNTA1. Compared with WT-SNTA1, p.P74LSNTA1 alone, and p.P74L/p.A257G-SNTA1, p.A257G-SNTA1 significantly increased peak I_{Na} density as previously reported ($P < 0.05$). Neither p.P74L-SNTA1 alone nor the double variant p.P74L/p.A257G-SNTA1 had a significant difference in peak I_{Na} amplitude compared to WT (Figure 1A; Table 1). These data suggest that the abnormal increased peak I_{Na} caused by p.A257G is negatively regulated intragenically by p.P74L back to approximately WT level.

To assess the effects of these mutants on late I_{Na}, we measured the level of late I_{Na} after leak subtraction as a percentage of peak I_{Na} elicited by prolonged depolarization. However, p.P74L, p.A257G and p.P74L/p.A257G showed similar percentages of late I_{Na} as WT-SNTA1 (Table 1), suggesting that the direct interaction of these SNTA1 mutants with Nav1.5 does not affect late I_{Na}.

We analyzed the kinetic parameters of activation and inactivation for these 3 SNTA1 variants and compared these data with WT-SNTA1. The p.P74L-SNTA1 variant showed no significant difference in either activation or inactivation compared with WT-SNTA1. As previously reported, the LQTS-associated p.A257G-SNTA1 missense mutation caused a statistically significant hyperpolarizing shift in activation and had comparable inactivation parameters to WT, thus increasing the overlap of the activation and inactivation curves, and resulting in increased *window current*. However, for p.P74L/p.A257G-SNTA1 both activation and inactivation were significantly shifted toward the hyperpolarizing direction and reversed the increased channel availability caused by p.A257G, significantly decreasing the window current from p.A257G-SNTA1 alone (Figure 1B-1F; Table 1).

The recovery time from fast inactivation was analyzed by fitting the data with a double-exponential equation. p.A257G-SNTA1 showed an increase in the fast component of the time constant τ_f (1.99 ± 0.16 ms, n = 20) compared with WT (1.63 ± 0.10 ms, n = 17; $P = 0.04$) as previously reported,[18] but there was no significant difference in time constant (τ_f, τ_s) and fractional amplitudes between WT, p.P74L, and p.P74L/p.A257G (*data not shown*). Due to the shift of activation parameters, we analyzed the decay of the peak I_{Na} with 2-exponential fits of decay phase of macroscopic I_{Na}. There was no difference in either time constants (τ_f, τ_s) or fractional amplitudes of 2 components observed in all mutants.

Discussion

As previously reported, four cases out of a population-based cohort of 292 SIDS victims and three subjects out of 400 control subjects were heterozygous for the combined variants p.P74L-SNTA1 and p.A257G-SNTA1 in α1-syntrophin.[16,18] Given the frequency of these two variants, and that neither variant was found in isolation in the SIDS cohort nor in the 400 reported adult controls, it is extremely likely that they are located on the same allele. Conversely, the p.A257G mutation without the p.P74L variant was found in isolation in three patients with LQTS.[18] No other putative cardiac channelopathic gene mutations had been identified previously in these 4 SIDS victims.[11,13-15,20] Because of the anonymized nature of the SIDS study, determination of genetic variants as transmitted or *de novo* was not possible.

The novel finding in this study is that the intragenic p.P74L-SNTA1 variant distinctively abolished the increased peak I_{Na} caused by the LQTS-associated p.A257G-SNTA1 missense mutation, thus reconciling the pro-arrhythmic nature of the mutation p.A257G-SNTA1 with

its discovery in a presumably healthy population as well as in our SIDS cohort at a > 1% frequency. To the best of our knowledge, this is the first report elucidating the functional interaction of a LQTS-associated SNTA1 mutation with an intragenic SNTA1 polymorphism.

Our group recently identified that the LQTS-associated SNTA1 missense mutation p.A257G markedly accentuated peak I_{Na} through the interaction of SNTA1 with Nav1.5 independent of the nNOS-PMCA4b nitrosylation pathway.[18], The present investigation showed that the intragenic combination of p.P74L-SNTA1 and p.A257G-SNTA1 significantly reverses the increased peak I_{Na} associated with p.A257GSNTA1 alone, and exerts an additional channel kinetic modification (negative shift for inactivation) on Nav1.5. The biophysical phenotype of normalized peak I_{Na} in p.P74L/p.A257G suggests that p.P74L plays a protective role, and could account for the persistence of p.P74L/p.A257G in the general population. Meanwhile, it also suggests that like the vast majority of SIDS cases, the pathogenic cause of the 4 SIDS cases with this combined variant remains elusive and the p.P74L/p.A257G combined variant did not contribute to their demise.

Notably, the two variants occurred on either side of the PDZ domain of SNTA1 (Figure 2). Specifically, p.P74L localizes to the first pleckstrin homology 1 (PH1) domain (amino acids 1-86) while p.A257G localizes to the second PH1 domain (amino acids 171-269). At the sarcolemma of the skeletal and cardiac muscles, SNTA1, the most abundant syntrophin isoform in heart muscle,[21,22] was shown to interact through its PDZ domain with many transmembrane channels such as sodium channels SkM1, SkM2, and Nav1.5,[23,24] potassium channel Kir4.1,[25] and transient receptor potential channels (TRPC).[26] More recently, the N-terminal part of SNTA1 containing the PDZ domain was confirmed to be necessary for SNTA1 to normally regulate TRPC1 channel[27] as well as to interact with the α_{1D}-adrenergic receptor.[28] Given its prominent modification of the biophysical phenotype, this interesting combined variation in the PH1 domain surrounding the PDZ domain provides us at least two questions to be further addressed: i) Is the PH1 domain necessary for a functional interaction between SNTA1 and Nav1.5? ii) Do these SNTA1 variants also have special effects on other proteins with PDZ binding sites in the Nav1.5 macromolecular complex *in vivo*?

In this study, we report for the first time an instance of intragenic complementation modulating the pathogenic phenotype of a mutation in a channelopathy-susceptibility gene. In particular, the functional characterization of the combination variant p.P74L/p.A257G-SNTA1 found in both SIDS and controls demonstrates an intragenic interaction of these two single nucleotide changes in SNTA1 by which the p.A257G mutant phenotype is abolished. To our knowledge, that an arrhythmia-associated mutation, namely p.A257G-SNTA1, in a ChIP is rescued by another intragenic variant has not been previously reported. However, this is certainly not the first report of this biological phenomenon. A common example in the cancer literature is the tumor suppressor p53, often mutated in cancer cells, in which the intragenic polymorphism R72P affects multiple p53 antitumor properties as well as drug response in a p53 mutation-dependent manner.[29-31]

To what extent this interaction is important in a more native cardiac environment as opposed to a heterologous expression system will need to be explored. However, it should be emphasized that the p.A257G-SNTA1 mutant phenotype appears to be nitrosylation-independent, since pathogenic changes were noted in a heterologous system without the presence of nNOS or PMCA4b, consistent with previous data.[18] These changes were abrogated in the presence of p.P74L without recapitulating the nitrosylation complex. Indeed, these findings present a mounting challenge in terms of properly recapitulating the proper sodium channel macromolecular complex for performing such studies. Given the increasing evidence of the interplay between genetic variation among various subunits,

caution must be exercised in properly interpreting such data not only from heterologous systems but indeed from any system that attempts to artificially recapitulate a mutant phenotype. An additional limitation to the present study is the lack of high-integrity RNA material to demonstrate the existence of p.P74L and p.A257G on the same SNTA1 allele. However, neither variant was identified in isolation in either our SIDS cohort or the controls examined. In addition, p.A257G was identified in the previous study in isolation only in LQTS-positive individuals, and p.P74L was not detected in those individuals. Thus it is extremely unlikely in control populations that p.A257G would exist in isolation rather than in linkage disequilibrium with a protective variant. Therefore, the current data support the previously argued pathogenic role of p.A257GSNTA1 when found in isolation without the accompanying polymorphism p.P74L-SNTA1.

In conclusion, this study highlights the complicated mechanism by which SNTA1 regulates Nav1.5, and emphasizes the potential role of genetic variation in Nav1.5 macromolecular complex-related disorders, as well as the increasingly complicated role that the individual genetic fingerprint plays in modulating the penetrance/expressivity of disease-associated mutations.

Acknowledgments

Funding: this work was supported by the University of Wisconsin Cellular and Molecular Arrhythmia Research Program (J.C.M.), the Mayo Clinic Windland Smith Rice Comprehensive Sudden Cardiac Death Program (M.J.A.), and grants HD42569 (M.J.A.) and HL71092 (J.C.M.) from the NIH, USA, and grants 30973367 and 81172901 (J.C.) from National Natural Science Foundation of China.

References

1. Schwartz PJ, Crotti L. Ion channel diseases in children: manifestations and management. Curr Opin Cardiol. 2008; 23:184–91. [PubMed: 18382205]
2. Ackerman MJ. The long QT syndrome: ion channel diseases of the heart. Mayo Clin Proc. 1998; 73:250–69. [PubMed: 9511785]
3. Splawski I, Shen J, Timothy KW, et al. Spectrum of mutations in long-QT syndrome genes. KVLQT1, HERG, SCN5A, KCNE1, and KCNE2. Circulation. 2000; 102: 1178–85. [PubMed: 10973849]
4. Tester DJ, Will ML, Haglund CM, Ackerman MJ. Compendium of cardiac channel mutations in 541 consecutive unrelated patients referred for long QT syndrome genetic testing. Heart Rhythm. 2005; 2:507–17. [PubMed: 15840476]
5. Wang Q, Curran ME, Splawski I, et al. Positional cloning of a novel potassium channel gene: KVLQT1 mutations cause cardiac arrhythmias. Nat Genet. 1996; 12: 17–23. [PubMed: 8528244]
6. Curran ME, Splawski I, Timothy KW, et al. A molecular basis for cardiac arrhythmia: HERG mutations cause long QT syndrome. Cell. 1995; 80:795–803. [PubMed: 7889573]
7. Wang Q, Shen J, Splawski I, et al. SCN5A mutations associated with an inherited cardiac arrhythmia, long QT syndrome. Cell. 1995; 80:805–11. [PubMed: 7889574]
8. Schwartz PJ, Stramba-Badiale M, Segantini A, et al. Prolongation of the QT interval and the sudden infant death syndrome. N Engl J Med. 1998; 338:1709–14. [PubMed: 9624190]
9. Schwartz PJ, Priori SG, Dumaine R, et al. A molecular link between the sudden infant death syndrome and the long-QT syndrome. N Engl J Med. 2000; 343:262–7. [PubMed: 10911008]
10. Brugada R, Hong K, Dumaine R, et al. Sudden death associated with short-QT syndrome linked mutations in HERG. Circulation. 2004; 109:30–5. [PubMed: 14676148]
11. Tester DJ, Ackerman MJ. Sudden infant death syndrome: how significant are the cardiac channelopathies? Cardiovasc Res. 2005; 67:388–96. [PubMed: 15913580]
12. Arnestad M, Crotti L, Rognum TO, et al. Prevalence of long-QT syndrome gene variants in sudden infant death syndrome. Circulation. 2007; 115:361–7. [PubMed: 17210839]

13. Cronk LB, Ye B, Kaku T, et al. Novel mechanism for sudden infant death syndrome: persistent late sodium current secondary to mutations in caveolin-3. Heart Rhythm. 2007; 4:161–6. [PubMed: 17275750]

14. Tester DJ, Dura M, Carturan E, et al. A mechanism for sudden infant death syndrome (SIDS): stress-induced leak via ryanodine receptors. Heart Rhythm. 2007; 4:733–9. [PubMed: 17556193]

15. Van, Norstrand DW.; Valdivia, CR.; Tester, DJ., et al. Molecular and functional characterization of novel glycerol-3-phosphate dehydrogenase 1 like gene (GPD1-L) mutations in sudden infant death syndrome. Circulation. 2007; 116:2253–9. [PubMed: 17967976]

16. Cheng J, Van Norstrand DW, Medeiros-Domingo A, et al. a-1 syntrophin mutations identified in sudden infant death syndrome cause an increase in late cardiac sodium current. Circ Arrhythmia Electrophysiol. 2009; 2:667–76.

17. Ueda K, Valdivia CR, Medeiros-Domingo A, et al. Syntrophin mutation associated with long QT syndrome through activation of the nNOS-SCN5A macromolecular complex. Proc Natl Acad Sci U S A. 2008; 105: 9355–60. [PubMed: 18591664]

18. Wu G, Ai T, Kim JJ, et al. Alpha-1-syntrophin mutation and the long-QT syndrome: a disease of sodium channel disruption. Circ Arrhythmia Electrophysiol. 2008; 1:193–201.

19. Nagatomo T, Fan Z, Ye B, et al. Temperature dependence of early and late currents in human cardiac wild- type and long Q-T DeltaKPQ Na+ channels. Am J Physiol. 1998; 275:H2016–24. [PubMed: 9843800]

20. Ackerman MJ, Siu BL, Sturner WQ, et al. Postmortem molecular analysis of SCN5A defects in sudden infant death syndrome. JAMA. 2001; 286:2264–9. [PubMed: 11710892]

21. Adams ME, Butler MH, Dwyer TM, et al. Two forms of mouse syntrophin, a 58 kd dystrophin-associated protein, differ in primary structure and tissue distribution. Neuron. 1993; 11:531–40. [PubMed: 7691103]

22. Adams ME, Dwyer TM, Dowler LL, et al. Mouse alpha 1- and beta 2-syntrophin gene structure, chromosome localization, and homology with a discs large domain. J Biol Chem. 1995; 270:25859–65. [PubMed: 7592771]

23. Gavillet B, Rougier JS, Domenighetti AA, et al. Cardiac sodium channel Nav1.5 is regulated by a multiprotein complex composed of syntrophins and dystrophin. Circ Res. 2006; 99:407–14. [PubMed: 16857961]

24. Gee SH, Madhavan R, Levinson SR, et al. Interaction of muscle and brain sodium channels with multiple members of the syntrophin family of dystrophin-associated proteins. J Neurosci. 1998; 18:128–37. [PubMed: 9412493]

25. Connors NC, Adams ME, Froehner SC, Kofuji P. The potassium channel Kir4.1 associates with the dystrophin-glycoprotein complex via alpha-syntrophin in glia. J Biol Chem. 2004; 279:28387–92. [PubMed: 15102837]

26. Vandebrouck A, Sabourin J, Rivet J, et al. Regulation of capacitative calcium entries by alpha1-syntrophin: association of TRPC1 with dystrophin complex and the PDZ domain of alpha1-syntrophin. FASEB J. 2007; 21:608–17. [PubMed: 17202249]

27. Sabourin J, Lamiche C, Vandebrouck A, et al. Regulation of TRPC1 and TRPC4 cation channels requires an alpha-syntrophin-dependent complex in skeletal mouse myotubes. J Biol Chem. 2009; 284:36248–61. [PubMed: 19812031]

28. Lyssand JS, DeFino MC, Tang XB, et al. Blood pressure is regulated by an alpha1Dadrenergic receptor/dystrophin signalo-some. J Biol Chem. 2008; 283:18792–800. [PubMed: 18468998]

29. Marin MC, Jost CA, Brooks LA, et al. A common polymorphism acts as an intragenic modifier of mutant p53 behaviour. Nat Genet. 2000; 25:47–54. [PubMed: 10802655]

30. Vikhanskaya F, Siddique MM, Kei Lee M, et al. Evaluation of the combined effect of p53 codon 72 polymorphism and hotspot mutations in response to anticancer drugs. Clin Cancer Res. 2005; 11:4348–56. [PubMed: 15958617]

31. Whibley C, Pharoah PD, Hollstein M. p53 polymorphisms: cancer implications. Nat Rev Cancer. 2009; 9:95–107. [PubMed: 19165225]

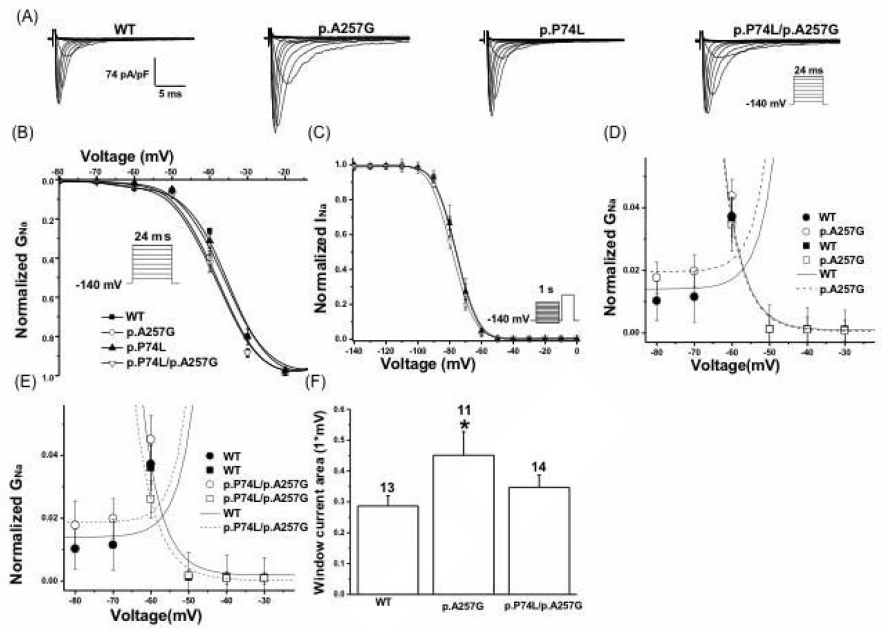

Figure 1.

Co-transfection of SNTA1 with SCN5A. A) Representative whole-cell current traces of HEK293 cells co-expressing WT or mutant SNTA1 and SCN5A, showing increased peak I_{Na} for p.A257G-SNTA1. The currents were recorded at membrane potentials between -120 to +60 mV in 10-mV increments from a holding potential of -140 mV as depicted in the protocol inset. B) Activation was measured using this protocol: currents were elicited by step depolarization for 24 ms to different potentials between −120 mV to 60 mV from a holding potential of −140 mV. The curves were fit with a Boltzmann function where $G_{Na} = [1+\exp (V_{1/2} - V) / K]^{-1}$, where $V_{1/2}$ and k are the midpoint and slope factor, respectively. $G/G_{Na} = I_{Na}$ (norm)/ (V - Vrev) where Vrev is the reversal potential and V is the membrane potential. p.A257G- and p.P74L/p.A257G-SNTA1 mutations caused a statistically significant hyperpolarizing shift in steady-state activation by 2.1-2.7 mV. C) Steady-state availability from inactivation was measured using the protocol shown in the inset and was determined by fitting the data to the Boltzmann function: $I_{Na} = I_{Na\text{-}Max} [1+\exp (Vc - V_{1/2}) / K]^{-1}$, where $V_{1/2}$ and k are the midpoint and the slope factor, respectively, and Vc is the membrane potential. p.P74L/p.A257G-SNTA1 mutation had a statistically significant hyperpolarizing shift in steady-state inactivation by 2.6 mV. D) The peak current activation data are replotted as a conductance (*G*) curve with steady-state inactivation relationships to show p.A257G increases the overlap of these relationships (window current). E) The peak current activation data are replotted as a conductance (*G*) curve with steady-state inactivation relationships to show p.P74L/p.A257G reverses the increased overlap of these relationships. Circles indicate activation, whereas squares indicate inactivation. Lines represent fits to Boltzmann equations with parameters of the fit and n numbers in Table 1. F) shows an increase in quantified window current area for p.A257G-SNTA1 compared with both WT-SNTA1 as well as p.P74L-p.A257G-SNTA1. *P<0.05 compared with WT and p.P74L/p.A257G. The experiment numbers are shown within each bar.

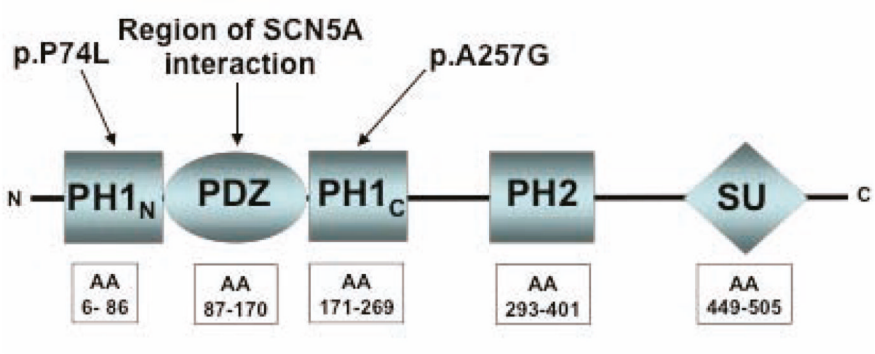

Figure 2.
Localization of SNTA1 variants. Illustrated is the linear topology for SNTA1 with variant localization.

Table 1

Electrophysiological properties of sodium channels in HEK293 cells co-expressing SCN5A and SNTA1.

Samples	Peak I_{Na}*		Activation			Inactivation			Late I_{Na}	
	pA/pF	n	V1/2(mV)	K	n	V1/2(mV)	K	n	%	n
WT-SNTA1	−169±13	28	−35.2±0.8	4.1	21	−75.8±0.9	4.8	27	0.159±0.05	18
p.A257G-SNTA1	−275±26°	27	−37.3±0.7°	3.8	19	−76.1 ±0.8	4.7	25	0.157±0.04	18
p.P74L-SNTA1	−204±17#	25	−36.0±0.6	4.0	13	−75.7±1.0	4.7	25	0.152±0.04	19
p.P74L/p.A257G-SNTA1	−194±23#	26	−37.9±0.8°	3.9	17	−78.4±1.0°#	4.9	26	0.120±0.04	10

*I_{Na} = Sodium current.

°$P < 0.05$ versus WT-SNTA1.

#$P < 0.05$ versus p.A257G-SNTA1. V1/2, pA/pF, and % Late I_{Na} are shown as the mean value and the standard error of the mean while K parameters are given as mean value.